Biomedical Optics EXPRESS

Three-wavelength light control of freely moving *Drosophila Melanogaster* for less perturbation and efficient social-behavioral studies

Yen-Yin Lin,[1,2,3,10,*] Ming-Chin Wu,[1,10] Po-Yen Hsiao,[4,10] Li-An Chu,[4] Mei-Mei Yang,[5] Chien-Chung Fu,[1,6,7,11] and Ann-Shyn Chiang[1,4,8,9]

[1]*Brain Research Center, National Tsing Hua University, Hsinchu 30013, Taiwan*
[2]*Institute of Photonics Technologies, National Tsing Hua University, Hsinchu 30013, Taiwan*
[3]*Department of Electrical Engineering, National Tsing Hua University, Hsinchu 30013, Taiwan*
[4]*Institute of Biotechnology, National Tsing Hua University, Hsinchu 30013, Taiwan*
[5]*Department of Art and Creative Design, Hsuan Chuang University, Hsinchu 30013, Taiwan*
[6]*Department of Power Mechanical Engineering, National Tsing Hua University, Hsinchu 30013, Taiwan*
[7]*Institute of Nanotechnology and Microsystems Engineering, National Tsing Hua University, Hsinchu 30013, Taiwan*
[8]*Genomics Research Center, Academia Sinica, Nankang, Taipei 11529, Taiwan*
[9]*Kavli Institute for Brain and Mind, University of California, San Diego, La Jolla, CA 92093-0526, USA*
[10]*These authors contributed equally to this work.*
[11]*ccfu@mx.nthu.edu.tw*
**yylin@ee.nthu.edu.tw*

Abstract: We developed a real-time automated laser-tracking system combined with continuous wave 1064-nm infrared or 473-nm blue lasers to provide punishment for studying memory in *Drosophila Melanogaster*. Combining optogenetic tools with laser properties, such as 473-nm and 593-nm lasers that activate light sensitive proteins in artificial transgenic flies, we can manipulate the specific neuron of an assigned fly among multiple flies to investigate neuron circuit relationships in social interactions. In restraining condition assay or optogenetic experiments, a ventral irradiated system would be more efficient due to higher ventral cuticle transmissions and neuron ganglia locations. Therefore, ventral irradiated systems cause less perturbation during behavior studies.

OCIS codes: (100.5010) Pattern recognition; (170.3660) Light propagation in tissues; (170.2655) Functional monitoring and imaging; (170.1420) Biology.

References and links

1. M. Bresadola, "Medicine and science in the life of Luigi Galvani (1737-1798)," Brain Res. Bull. **46**(5), 367–380 (1998).
2. K. J. T. Venken, J. H. Simpson, and H. J. Bellen, "Genetic manipulation of genes and cells in the nervous system of the fruit fly," Neuron 72, October 20, 2011.
3. R. L. Fork, "Laser stimulation of nerve cells in Aplysia," Science **171**(3974), 907–908 (1971).
4. G. Nagel, T. Szellas, W. Huhn, S. Kateriya, N. Adeishvili, P. Berthold, D. Ollig, P. Hegemann, and E. Bamberg, "Channelrhodopsin-2, a directly light-gated cation-selective membrane channel," Proc. Natl. Acad. Sci. U.S.A. **100**(24), 13940–13945 (2003).
5. K. Deisseroth, G. Feng, A. K. Majewska, G. Miesenböck, A. Ting, and M. J. Schnitzer, "Next-generation optical technologies for illuminating genetically targeted brain circuits," J. Neurosci. **26**(41), 10380–10386 (2006).
6. E. S. Boyden, F. Zhang, E. Bamberg, G. Nagel, and K. Deisseroth, "Millisecond-timescale, genetically targeted optical control of neural activity," Nat. Neurosci. **8**(9), 1263–1268 (2005).
7. C. Schroll, T. Riemensperger, D. Bucher, J. Ehmer, T. Völler, K. Erbguth, B. Gerber, T. Hendel, G. Nagel, E. Buchner, and A. Fiala, "Light-induced activation of distinct modulatory neurons triggers appetitive or aversive learning in *Drosophila* larvae," Curr. Biol. **16**(17), 1741–1747 (2006).
8. K. Inada, H. Kohsaka, E. Takasu, T. Matsunaga, and A. Nose, "Optical dissection of neural circuits responsible for *Drosophila* larval locomotion with halorhodopsin," PLoS ONE **6**(12), e29019 (2011).
9. G. S. Suh, S. Ben-Tabou de Leon, H. Tanimoto, A. Fiala, S. Benzer, and D. J. Anderson, "Light activation of an innate olfactory avoidance response in *Drosophila*," Curr. Biol. **17**(10), 905–908 (2007).
10. M.-C. Wu, L.-A. Chu, P. Y. Hsiao, Y.-Y. Lin, C.-C. Chi, T.-H. Liu, C.-C. Fu, and A. S. Chiang, "Optogenetic control of selective neural activity in multiple freely moving *Drosophila* adults," Proc. Natl. Acad. Sci. U.S.A. **111**(14), 5367–5372 (2014).

#228628 - $15.00 USD Received 26 Nov 2014; revised 31 Dec 2014; accepted 31 Dec 2014; published 13 Jan 2015

11. J.-N. Yih, Y. Y. Hu, Y. D. Sie, L.-C. Cheng, C.-H. Lien, and S.-J. Chen, "Temporal focusing-based multiphoton excitation microscopy via digital micromirror device," Opt. Lett. **39**(11), 3134–3137 (2014).
12. A. M. Leifer, C. Fang-Yen, M. Gershow, M. J. Alkema, and A. D. Samuel, "Optogenetic manipulation of neural activity in freely moving Caenorhabditis elegans," Nat. Methods **8**(2), 147–152 (2011).
13. H. Dankert, L. Wang, E. D. Hoopfer, D. J. Anderson, and P. Perona, "Automated monitoring and analysis of social behavior in *Drosophila*," Nat. Methods **6**(4), 297–303 (2009).
14. J. R. Trimarchi and A. M. Schneiderman, "Giant fiber activation of an intrinsic muscle in the mesothoracic leg of *Drosophila melanogaster*," J. Exp. Biol. **177**, 149–167 (1993).
15. F. Zhang, L.-P. Wang, M. Brauner, J. F. Liewald, K. Kay, N. Watzke, P. G. Wood, E. Bamberg, G. Nagel, A. Gottschalk, and K. Deisseroth, "Multimodal fast optical interrogation of neural circuitry," Nature **446**(7136), 633–639 (2007).
16. S. S. Bidaye, C. Machacek, Y. Wu, and B. J. Dickson, "Neuronal control of *Drosophila* walking direction," Science **344**(6179), 97–101 (2014).
17. J. Y. Lin, P. M. Knutsen, A. Muller, D. Kleinfeld, and R. Y. Tsien, "ReaChR: a red-shifted variant of channelrhodopsin enables deep transcranial optogenetic excitation," Nat. Neurosci. **16**(10), 1499–1508 (2013).
18. H. K. Inagaki, Y. Jung, E. D. Hoopfer, A. M. Wong, N. Mishra, J. Y. Lin, R. Y. Tsien, and D. J. Anderson, "Optogenetic control of *Drosophila* using a red-shifted channelrhodopsin reveals experience-dependent influences on courtship," Nat. Methods **11**(3), 325–332 (2013).
19. S. Yamaguchi, C. Desplan, and M. Heisenberg, "Contribution of photoreceptor subtypes to spectral wavelength preference in *Drosophila*," Proc. Natl. Acad. Sci. U.S.A. **107**(12), 5634–5639 (2010).
20. D. E. Bath, J. R. Stowers, D. Hörmann, A. Poehlmann, B. J. Dickson, and A. D. Straw, "FlyMAD: Rapid thermogenetic control of neuronal activity in freely walking *Drosophila*," Nat. Methods **11**(7), 756–762 (2014).

1. Introduction

Manipulating neuron cells *in vivo* is an important approach in neuroscience research for understanding major functions of specific neuron circuits. In the 1780s, Luigi Galvani discovered that an electric current could be used to stimulate neurons artificially [1]. This discovery inspired artificial neuron manipulation through optical, chemical, mechanical, and thermal means [2]. Although several methods of stimulating neurons have been demonstrated, microelectrodes are still necessary for manipulating and monitoring neurons at an acceptable spatial resolution and specificity. In 1971, the optical approach was demonstrated, and lasers can provide superior spatial and temporal resolution [3]. One significant drawback of the optical method is a lack of specificity between various neurons; however, state-of-the-art genetically modified animals can help the optical method target specific neural circuits. Therefore, the resolution and specificity can be simultaneously satisfied in optical-based systems. This approach, which is known as optogenetic technology, can be used to investigate intact, living neural circuits [4–6].

To understand the causal relationship between neural circuits and behavioral phenotypes, neuroscientists have created many behavioral assays using implanted optogenetic tools that monitor excitatory and/or inhibitory signals at the millisecond scale to record specific behavioral responses of fruit fly larvae [7, 8], fruit fly adults [9], and one specific adult fly among multiple flies [10]. From these exciting results, we realize that non-invasive, versatile, economical behavioral machines will help scientists screen behavior-related neuron circuits. In the present work, we improved our previous automated laser tracking and optogenetic manipulation system (ALTOMS) [10]. First, we found that ventral irradiation requires reduced laser intensity compared to dorsal irradiation. To produce a more economical system, we replace the delicate notch filters with a long-pass filter and report the error rate of this modified system. Finally, we extend this system from a two-color system to a three-color system by including 1064-nm IR laser as a punishment in order to exclude visual effects. Therefore, this system can deliver punishment and simultaneously activate channelrhodopsin-2 (ChR2) and a red-shifted variant of channelrhodopsin (ReaChR). Both digital micro-mirror device (DMD) and galvo motors can direct laser beam to assigned positions. The most attractive features of DMD include an ability to generate arbitrary illumination patterns and compatibility with an incoherent light source. DMD also acts as a two-dimensional diffraction grating [11], so an image-system is necessary to convert blurred patterns into focused illumination patterns. Another interesting feature of DMD is that the power of the light source distributes over several millions pixels, so the maximum power of each pixel is much less than the total power. These attributes make DMD a perfect tool for microscope-based

#228628 - $15.00 USD Received 26 Nov 2014; revised 31 Dec 2014; accepted 31 Dec 2014; published 13 Jan 2015

behavioral assays [12]. Galvo motors can provide just a single illumination point, so the maximum power of illumination point equals that of the used laser source; hence, ALTOMS can provide punishment stimulus with a collimated laser beam.

2. Differences between dorsal and ventral irradiation

The *Drosophila* cuticle provides protection against body fluid evaporation, sunshine, and mechanical damages; however, optical transmission of the cuticle is not homogeneous due to variations in pigment concentration and the difference in the cuticle structure between the dorsal and ventral body segments. Therefore, optical transmission of the cuticle was measured in six regions: dorsal anterior head, dorsal thorax, dorsal abdomen, ventral abdomen, ventral posterior head, and proboscis. Figure 1(A) shows the corresponding anatomical regions, which are marked by different colors. The transmission curves of dissected cuticle samples were measured using a micro-spot spectroscopic ellipsometer (J. A. Woollam M-2000U). The measurement results were normalized to the 473-nm transmission of ventral abdomen. As the dissected cuticles samples were sandwiched between two 150-μm glass cover slides, wavelengths shorter than 350 nm were absorbed by the glass cover slides. Figure 1(B) shows the transmissions of the cuticle samples plotted against wavelength from 350 nm to 1000 nm; the transmission at longer wavelengths is better due to lower scattering losses. The experimental results show that samples from the ventral side have higher transmission than those from the dorsal side.

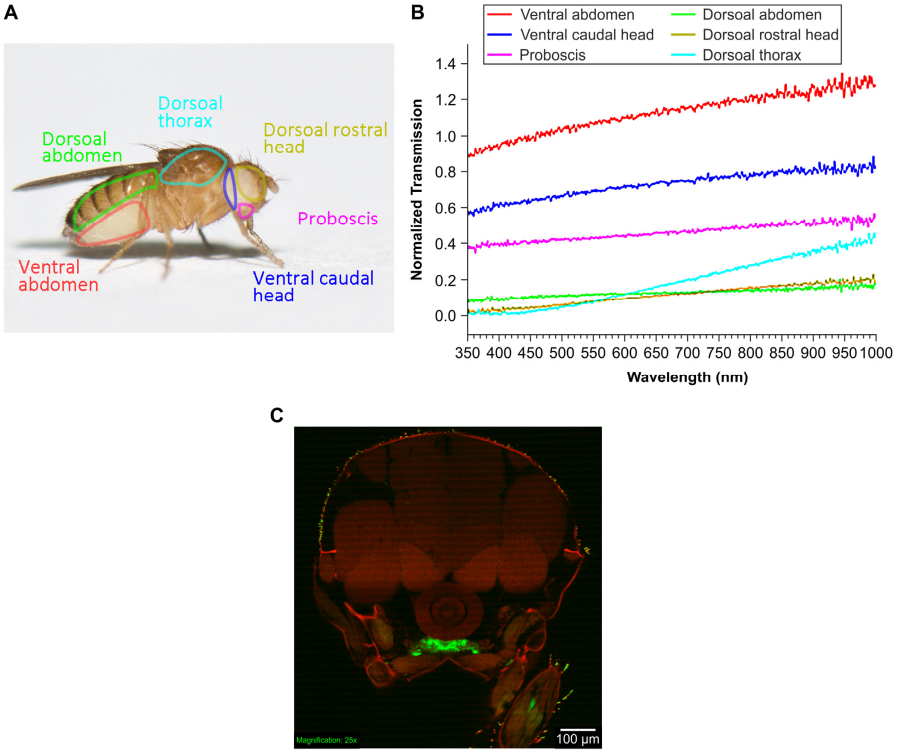

Fig. 1. (A) Fruit fly anatomy. (B) Optical transmission of different anatomical regions. The measurement results were normalized to the ventral abdomen value at 473 nm, which showed a 33% transmission. (C) The confocal image of the thoracic ganglia in the transverse section of the *Elav-Gal4 > UAS-GFP* fly at the second pair of legs. The white scale bar represents 100 μm.

The nervous systems of various insects show diverse ganglia arrangements, which are commonly located in the ventral nerve cord. Figure 1(C) shows the confocal image of thoracic ganglia in the transverse section of the pan-neuronal *Elav-Gal4 > UAS-GFP* fly, which

#228628 - $15.00 USD Received 26 Nov 2014; revised 31 Dec 2014; accepted 31 Dec 2014; published 13 Jan 2015

expresses the ventral nerve cord. Here, green represents the neurons labeled with green fluorescent protein (GFP), while red represents the auto-fluorescence of unlabeled tissues. Figure 1(C) reveals that the neurons are mostly located at the ventral side. Both the transmission of cuticle samples and the location of neuron ganglia suggest that ventral irradiation is the preferred arrangement for the modified ALTOMS.

3. Ventral irradiation ALTOMS

3.1 System configuration

The ventral irradiation ALTOMS is composed of four parts: arena, image capture module (ICM), laser scanning module (LSM), and intelligent central-control module (ICCM). The schematic and photograph of the modified ALTOMS are shown in Fig. 2(A) and 2(B), respectively.

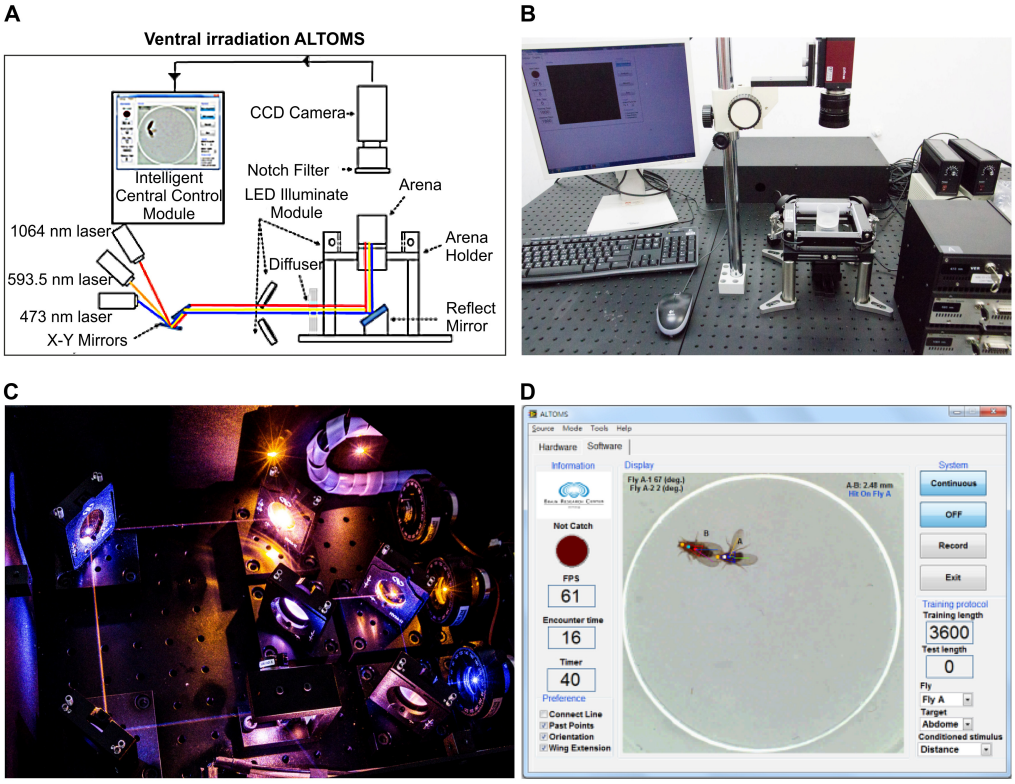

Fig. 2. The ventral irradiation ALTOMS (A) schematic and (B) photograph. (C) A photo of the LSM for the ventral irradiation ALTOMS. (D) Graphical user interface with five regions: information, preferences, display, system, and training protocol. The CCD camera with two-notch filter captures image without color distortion.

The arena has a diameter of 20 mm and a height of 3 mm. The coarse sidewalls of the arena help provide uniform light irradiation and improved image contrast between the targets and the background. Furthermore, the arena is covered with anti-reflective glass coated with water repellent to deter flies from clinging to the surface [13]. The arena is advantageous for ventral irradiation ALTOMS because both the bottom and cover are transparent to laser irradiation and image-taping. The ICM consists of a charge-coupled device (CCD) camera (AVT^{TM} Pike F-032) and a white LED illuminator (EXLITE DAL-15-100-4-W). The ICM can record videos with 640 × 480 pixels per frame at a rate of 208 frames per second (fps). The LSM consists of a pair of galvo motors (Cambridge Technology 6200H) with 130-μs small angle step response and three diode-pumped solid-state (DPSS) lasers: continuous wave

#228628 - $15.00 USD Received 26 Nov 2014; revised 31 Dec 2014; accepted 31 Dec 2014; published 13 Jan 2015

(cw) 473-nm blue laser, cw 593.5-nm yellow laser, and cw 1064-nm infrared (IR) laser. (Fig. 2(C)) Three independent computer-controlled mechanical shutters with 1-ms transfer time on opening modulate the laser by switching the laser on/off independently or simultaneously. The sizes of the collimated laser spots, which were measured at the arena by a beam profiler (DataRay Inc. BladeCam-HR CMOS Camera), were 1.1 mm, 1.05 mm, and 2 mm in diameter for the 473-nm, 593.5-nm, and 1064-nm lasers, respectively. The ICCM interactively controls the LSM by analyzing the online video with a 17-ms delay time from the captured image to targeting the assigned fly. The galvo motor's and the shutter's responses are much shorter than the image analysis delay, so a faster and more reliable image processing algorithm is the key requirement to improve the speed of ALTOMS. The software is capable of analyzing multiple fly positions, orientations, wing extension angles, and relative distances between flies. The user-friendly graphical user interface (GUI), shown in Fig. 2(D), assists biologists in setting comprehensive parameters, including training protocols, laser excitation duration, and position of laser irradiation. Therefore, this system potentially enables several new *Drosophilia* social behavioral assays.

In ventral irradiation ALTOMS, we attempted to use an economical long-pass filter (Thorlab FGL610, 610 nm long-pass color filter) to replace the two notch filters (Kaiser HNF-473.0, HNF-593.5) used in the first-generation ALTOMS [10]. Figure 2(D) displays the image of the CCD camera with the notch filters. The notch filters can block blue and yellow laser light without color distortion, but the total cost of two notch filters is about 20 times that of a long-pass color filter. Figure 3 shows the CCD camera with a long-pass filter. Clearly, the image contrast is poor compared to that shown in Fig. 2(D), and the color of the flies becomes similar to the background color. Therefore, the image-processing algorithm needs to be modified for ventral irradiation ALTOMS. The color image is obtained (Fig. 4(A)) and the red plane of the color image is converted into a gray-level image (Fig. 4(B)), ignoring both green and blue lights. The gray-level image is then converted into a binary image with an appropriate contrast value (Fig. 4(C)). Here, red represents 1, which is a bright background, whereas black represents 0, which is the fly. The inverse binary image was then obtained (Fig. 4(D)), allowing identification of the fly positions. To improve the image further, small particles are removed, and a noise filter is applied, as shown in Fig. 4(E). Finally, the position, orientation, and wing angle of each fly is calculated, and the relative distance or overlap between two flies is determined. The results are displayed in the GUI (Fig. 4(F)).

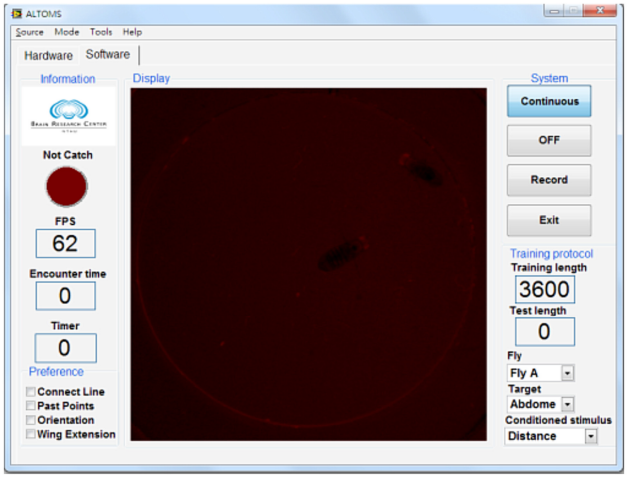

Fig. 3. The GUI Interface when the CCD camera with an economical 610nm longpass filter capture image. The brightness of the image is much lower.

#228628 - $15.00 USD Received 26 Nov 2014; revised 31 Dec 2014; accepted 31 Dec 2014; published 13 Jan 2015

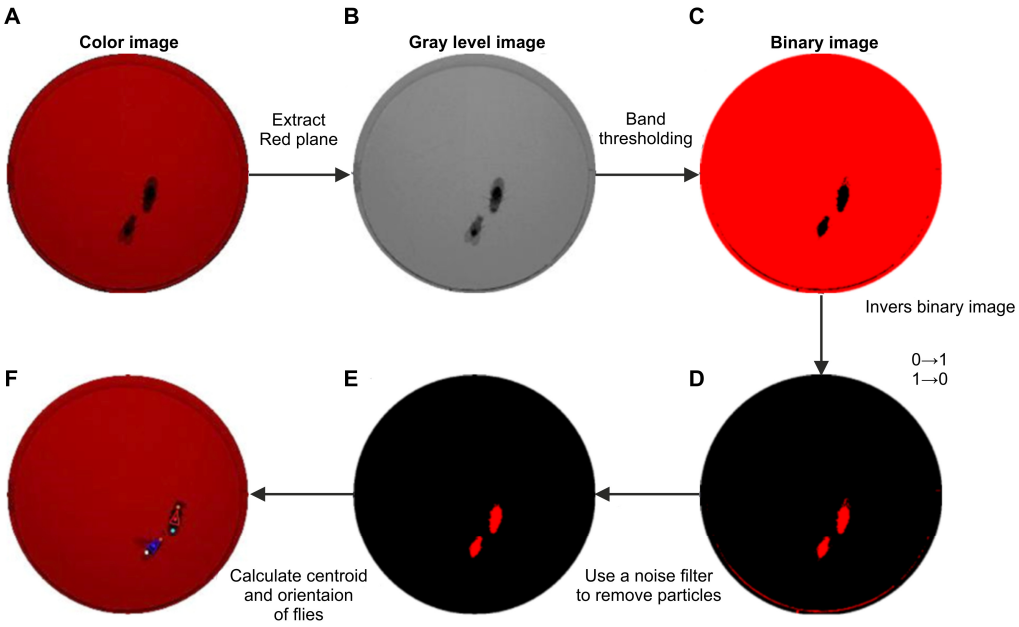

Fig. 4. Image processing steps. (A) Original color image from CCD camera. (B) Red plane extracted and the color image converted into gray-level image. (C) The gray-level image converted into a binary image using a long-pass filter. (D) The binary image is inversed. (E) Small particles removed and a particle filter applied on the "Area" function. Center of mass is calculated as an indicator of the fly positions. (F) After classification, all calculated results are labeled for each fly, including the position, orientation, and relative distance between two flies.

3.2 System validation

Occasional crossover of two flies during the experiment influences the precision of the real-time tracking of an identified male. Visual inspection of the recorded videos (30 minutes for the naïve male) showed that the error rate for the automated real-time analysis and tracking system was below 0.0071% in all image frames, as shown in Table 1. Moreover, the error rate of this economical system is similar to that of the notch filter system.

Table 1. Visual validation of system accuracy in tracking fly identities. In each assay, social interactions between a naïve male and virgin female were continuously videotaped for 30 min or until the beginning of copulation. Videos were recorded at 37 fps. Image frames containing flies within a relative distance of 3.5 mm were automatically detected. We visually inspected the number of incidents in which the system tracked the wrong individual after crossover between the two flies.

FPS = 37 observation period 30 min or stop by mating			
Test no.	Errors	Frames	Error/Frame (%)
1	5	49580	0.0101
2	4	28860	0.0139
3	4	66600	0.0060
4	5	66600	0.0075
5	1	15910	0.0063
6	4	66600	0.0060
7	2	36112	0.0055
8	1	66600	0.0015
Average error rate (%): 0.0071%			

Although we used the orientation in frame *t*-1 compared to the orientation in frame *t* to correct the orientation, the derived accuracy rate was only 59% (Table 2). These results included frequent exchanges of the head and tail; thus, we added the wing position to assist in orientation correction, which greatly improved the orientation judgments. Table 2 shows the

#228628 - $15.00 USD Received 26 Nov 2014; revised 31 Dec 2014; accepted 31 Dec 2014; published 13 Jan 2015

orientation accuracy rate when the wing position was included in the orientation correction. The accuracy rate increased from 59% to 94%.

Table 2. Accuracy rate of head and thorax irradiation.

2-s on / 4-s off 473-nm laser irradiation with 40-mW/mm^2 intensity	
Type	Accuracy rate over 150 on/off periods
Head without wing position assist	59.3%
Thorax without wing position assist	59.3%
Head with wing position assist	94%
Thorax with wing position assist	96%

4. Fly sample preparations and protocols

4.1 Flies in the restrained conditioning assay

In restraining conditioning experiments, a wild virgin female fly and a naïve male fly are present in the arena at the same time. During the 60-min training period, when the distance between the two flies was less than 3.5 mm (approximately a fly body length) for a meeting period of longer than 2 seconds, the laser (blue or IR), functioning as heat punishment, was directed at the male fly's abdomen until the distance between the flies was greater than 3.5 mm. The laser power was varied to compare the training effects between ventral and dorsal irradiation by observing the trained flies for 30 minutes.

4.2 ChR2 transgene flies for jumping and backward reflex assay

In the jumping or backward reflex assay, we genetically expressed both ChR2 proteins on the giant fiber (*12862-Gal4 > UAS-ChR2* or VT50660 > *UAS-ReaChR*). Half the *12862-Gal4 > UAS-ChR2* flies were fed standard food containing 100-μM all-*trans*-retinal for 7 days. For control, the remaining flies were fed standard food without all-*trans*-retinal for 7 days. The ChR2 protein does not function properly in flies of the control batch [4]. For the jumping reflex assay, the dorsal anterior head and ventral posterior head of each fly were targeted with a 473-nm laser and illuminated for 10 cycles of 3-s on-and-off intervals [10]. For the backward reflex assay, backward rates were determined during 15 cycles of 1-s on/9-s off 593.5-nm laser irradiation on the thorax of *VT50660-Gal4 > UAS-ReaChR* at different laser energies and irradiation directions.

5. Experimental results

5.1 Optogenetic experiment (Jumping reflex assay or backward reflex assay)

In this assay, transgenic flies which have been adopted in ref [10] expressed GFP on giant fiber neurons (Fig. 5(A)). Activation of the giant fibers also triggers the tibial levator, an intrinsic leg muscle, with a 1.46 ± 0.02-ms time-delay [13]. Thus, this phenotype can be used to examine our system. Figure 5(B) shows the jumping reflex rate plotted against different laser intensities, food type, and irradiation direction. As shown in Fig. 5(B), the jumping reflex rate of ventral irradiation ALTOMS is normally higher than dorsal irradiation ALTOMS. A minimum laser intensity of 3 mW/mm^2 can trigger the jumping reflex in a ventral irradiation ALTOMS (Fig. 5(B)). However, the jumping rate cannot reach 100% and is not significantly different between ventral and dorsal irradiation ALTOMS when the laser intensity is larger than 21 mW/mm^2 (Fig. 5(B)). Therefore, over-excitation can lead to saturation of the neuron response in optogenetic trigger jumping reflex experiments. As shown in Fig. 5(C), we can ventrally activate specific neurons with high-intensity blue laser (42 mW/mm^2). The *12862-Gal4 > UAS-ChR2* flies fed with all-*trans*-retinal jumped frequently when the laser irradiated the head and thorax but not when the abdomen was irradiated. When the high-intensity blue laser illuminated their abdomen, the flies simply avoided the blue laser and jumped a few times. Therefore, these results show that the jump behavior is due to giant fiber activation because the giant fibers are only distributed in the head and thorax, which are consistent with anatomical images (Fig. 5(A)).

#228628 - $15.00 USD Received 26 Nov 2014; revised 31 Dec 2014; accepted 31 Dec 2014; published 13 Jan 2015

Next, we evaluated the effectiveness of the optogenetic excitation of neural activity in living flies with the moonwalker descending neuron (MDN) expressing the red-activatable ChR (ReaChR) gene, which is optimally excited with an orange to red (590–630 nm) light-driven pump specific for Na^+ ions [15–18]. With pulse yellow (593.5 nm) laser irradiation of the thorax, we found that the experimental flies fed with all-*trans*-retinal exhibited significantly higher backward rate in ventral irradiation ALTOMS than dorsal irradiation ALTOMS (Fig. 5(D)). In this assay, the expression pattern of *VT50660-Gal4* transgenic flies is shown in Fig. 5(E).

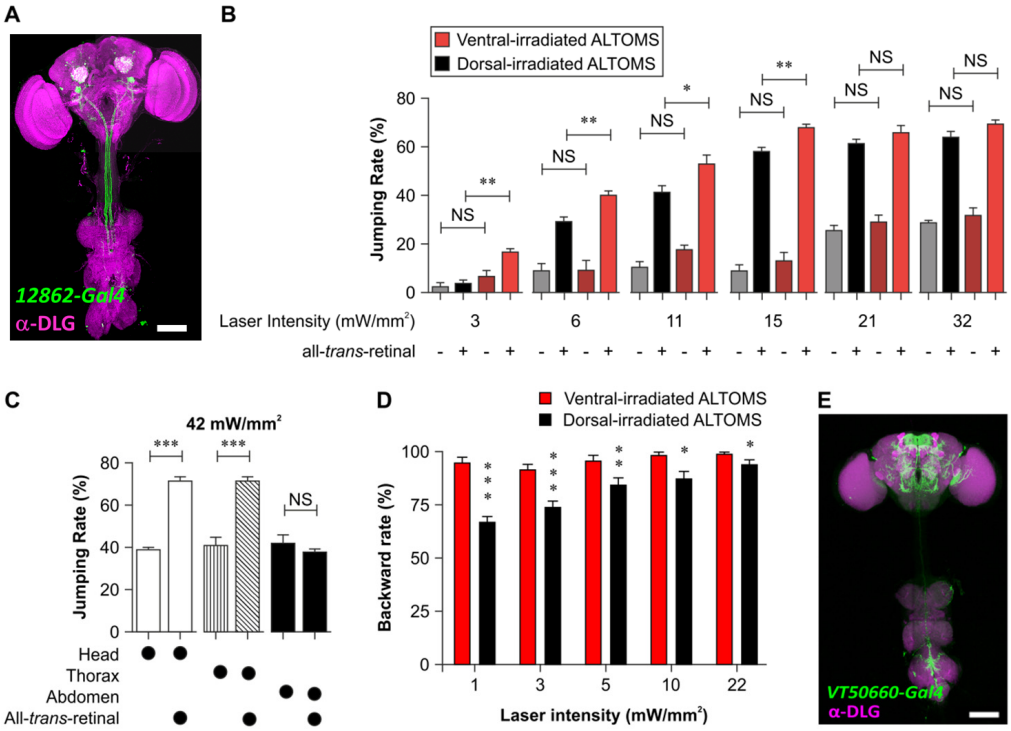

Fig. 5. (A) Giant fiber neurons (green) were preferentially labeled in the *12862-Gal4 > UAS-GFP* fly or (E) in the *VT50660-Gal4 > UAS-GFP* fly. The brain and thoracic ganglia were immunostained with anti-discs large antibody (magenta). Scale bar represents 100 μm. (B) Jumping rates during 10 cycles of 3-s on-off blue laser irradiation on the head and thorax at different laser energies and irradiation directions. (C) Jumping rates in *12862-Gal4 > UAS-ChR2* flies under 42-mW/mm^2 laser ventral irradiation of three different body parts. (D) Backward rates during 15 cycles of 1-s on/9-s off yellow irradiation on the thorax of *VT50660-Gal4 > UAS-ReaChR* at different laser energies and irradiation directions. (E) The expression pattern of VT50660-Gal4 transgenic flies. Scale bar represents 100 μm. In all experiments, each value represents mean ± SEM (N = 8), *P < 0.05, **P < 0.01, and ***P < 0.005.

5.2 Restrained conditioning assay

During a 60-min training period, when the distance between the two flies was shorter than 3.5 mm, the cw 1064-nm IR or cw 473-nm blue lasers are used as heat punishment to irradiate the male's head (Fig. 6(A)). During the 30-min test period without laser irradiation, we defined the restraining index (RI) for quantitatively discussing observation results:

$$\text{Restraining Index (RI)} = \frac{\text{Accumulated non-meeting (relative distance} > 3.5\text{ mm) time}}{\text{Total observation time}} \times 100\%. \quad (1)$$

From the definition of RI, a higher score represents superior training efficiency. Figure 6(B) shows the statistics from dorsal irradiation and ventral irradiation; the number N of each data

#228628 - $15.00 USD Received 26 Nov 2014; revised 31 Dec 2014; accepted 31 Dec 2014; published 13 Jan 2015

point is 5. This experiment can be divided into three groups. The first group includes untrained naïve flies (N = 8), the second group includes flies that were trained by ventral irradiation, and the last group includes flies that were trained by dorsal irradiation. For the naïve group, the average RI is 33.7% with 8.4% deviation. Both ventral and dorsal irradiation experiments show that the higher laser power can result in better training and that the flies can be trained against natural behavior. The ventral irradiation experiments required lower laser power to reach similar training effects. At RI < 90%, the minimum required laser power of the dorsal and ventral irradiation is 30 mW/mm^2 and 14 mW/mm^2, respectively. Although the decrease in the minimum required laser power is not inversely proportional to transmission data, these results still reflect that transmission to the ventral abdominal cuticle was superior to transmission to the dorsal abdominal cuticle. Thus, because the ventral side has more pain neurons, we can use a lower laser intensity to train flies compared to their dorsal side.

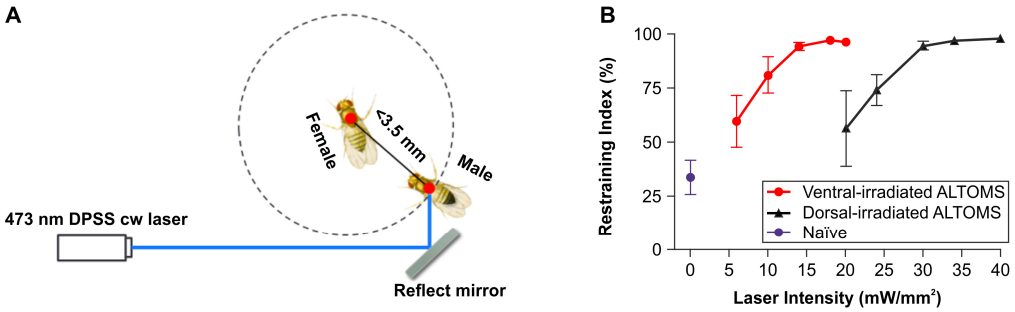

Fig. 6. (A) Schematic of a naïve male fly being irradiated when it is within 3.5 mm of the female for more than 2 s. (B) Restraining index of the 473-nm laser training effect versus different laser powers and irradiation directions (N = 8). Genotype: *wild-type Canton-S w1118*.

5.3 IR Laser for restrained conditioning assay

Since the blue (473 nm) laser is visible to a fly, the blue laser might induce aversive behavior when used as a punishment source. Pain and adverse behavior cannot be separated. These two factors could prevent researchers from determining the exact mechanism of the experimental results. According to previous reports [19], flies cannot sense light when the wavelength is longer than 600 nm. Therefore, we can replace the blue laser by a 1064-nm IR laser as a punishment source. To verify the effectiveness of the IR laser, we performed a 10-min experiment during which a single fly moved freely in an arena that was virtually divided into two equal halves by the ICCM (Fig. 7(A)), invisible to the fly. The fly was continuously irradiated by an IR laser (1064 nm) projected on a specified body part (head, thorax, or abdomen) at different intensities, whenever the fly entered the forbidden zone (FZ, left half of the arena). We found that flies rarely stayed in the FZ, when irradiated by an IR laser with intensity over 100 mW/mm^2 on any body part (Fig. 7(B)). Thus, the avoidance response was dependent on laser intensity. Figure 7(C) shows the RI for different laser intensities. The results show that a male fly trained with a 100-mW/mm^2 laser avoided a virgin female at a significantly higher RI than a naïve male, and the results are consistent with the safe/forbidden zone test. Because the IR laser (of intensity at least 100 mW/mm^2) requires a higher intensity to obtain good learning scores, we study the death rate of flies under different IR laser intensities, as shown in Fig. 7(D). When the IR laser intensity is lower than 120 mW/mm^2, we could not identify any flies killed by continuous IR laser irradiation. Therefore, the suggested IR punishment intensity is 100–120 mW/mm^2 for ventral irradiation ALTOMS.

#228628 - $15.00 USD Received 26 Nov 2014; revised 31 Dec 2014; accepted 31 Dec 2014; published 13 Jan 2015

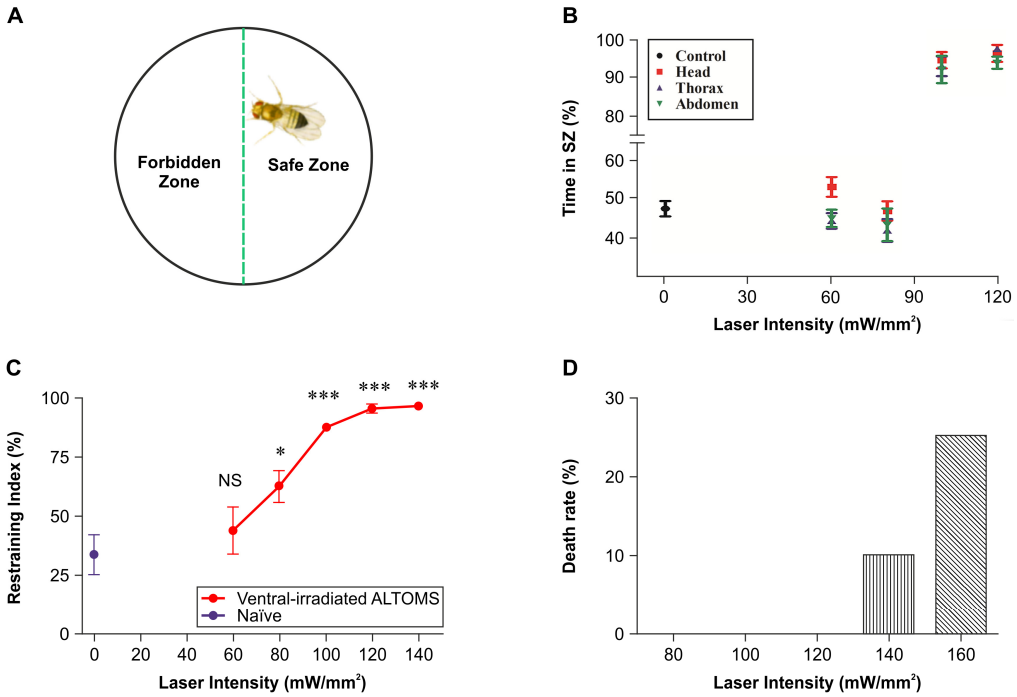

Fig. 7. (A) Virtual division of an arena into forbidden zone (FZ) and safe zone (SZ). (B) Distribution of a male fly in the arena during 10-min training (N = 8). (C) RI of IR laser training effects under multiple intensities. Data represent mean ± SEM (N = 8), *P < 0.05, **P < 0.01, and ***P < 0.005. (D) Death rates for different laser intensities (N = 8). Genotype: *wild-type Canton-S w1118*.

6. Summary

In this study, we proved that our automated laser tracking and optogenetic manipulation system (ALTOMS) is a versatile tool for *Drosophila* behavioral experiments. We integrated a three-wavelength laser scanning system and a real-time image analyzing system to punish a specific fly or to activate/inhibit specific neurons. We found that ventral laser irradiation was much more efficient than dorsal laser irradiation due to the higher transmission of the ventral cuticle and the locations of neuron ganglia. Here, we also demonstrated that intense IR laser radiation could also be used to train a male fly in the safe/forbidden zone test and restrained conditioning assay. Although the IR laser required higher laser intensity during training, the results showed that the IR laser punishment at 100–120 mW/mm^2 can properly train a male fly without killing it. However, the visual effects of IR laser punishment are reduced, and a suitable IR laser can sufficiently heat an adult fly to trigger temperature-sensitive silencers and activators [20]. Therefore, this system has the potential to contribute to a variety of *Drosophila* behavioral experiments. For example, our system could be used to systematically map memory circuits in a *Drosophila* brain.

Acknowledgments

This work was supported by grants from the Ministry of Science and Technology, the Ministry of Education and the Brain Research Center of the University System of Taiwan. We thank Klemens F. Störtkuhl, Barry J. Dickson, and David J. Anderson for providing flies. We thank Hsiang-Lin Liu for providing a micro-spot spectroscopic ellipsometer. We thank Hsiu-Ming Chang for his discussion and comments on the manuscript. We thank Chih-Wei Hsu for initial testing of the ChR2 experiments.